Sebastian STYŁA, Monika MAŃKO

Lublin University of Technology, Institute of Electrical Engineering and Electrotechnologies

doi:10.15199/48.2020.01.58

A reluctance model of an electromagnetic mill using the stator of an asynchronous motor as an inductor

***Abstract.** The construction of a mill using the stator of an asynchronous motor as an inductor is a prototype construction. The article attempts to develop a mathematical model of an electromagnetic mill based on reluctance networks. It presents the kinds of raw materials shredded in this sort of mill as well as granulometric distribution of a quartz sand. The possibilities of using the device in other applications are also proposed.*

Streszczenie.** Konstrukcja młyna wykorzystująca w roli wzbudnika stojan silnika asynchronicznego jest konstrukcją prototypową. W artykule dokonano próby opracowania modelu matematycznego młyna elektromagnetycznego opartego o sieci reluktancyjne. Ponadto przedstawiono grupy surowców rozdrabnianych w tego rodzaju młynie oraz zaprezentowano rozkład granulometryczny dla piasku kwarcowego. Zaproponowano także możliwości wykorzystania urządzenia w innych zastosowaniach. (**Model reluktancyjny młyna elektromagnetycznego wykorzystującego w roli wzbudnika stojan silnika asynchronicznego).

Keywords: electromagnetic mill, grinding, milling, reluctance, mathematical model.
Słowa kluczowe: młyn elektromagnetyczny, rozdrabnianie, mielenie, reluktancja, model matematyczny.

Introduction

Electrical machines, which include the electromagnetic mill in question, belong to complex physical objects. The development of an adequate mathematical model reflecting the relationships and dependencies between the individual circuits of the mill is extremely important from the point of view of the ability to estimate the properties and behaviour of the machine during the operation process. The mathematical model shown is based on reluctance networks. In this model the following areas are distinguished: inductor, air gap, working chamber and grinding media. Depending on the geometric dimensions and magnetic permeability of a given material and network division, it is possible to determine the reluctance of particular mill elements.

Electromagnetic mill

Grinding materials by means of electromagnetic field is a new, highly effective technology, developed by several research and development centres in Poland. The structures developed are based on inductors with open poles [1], [2], [3], [4].

Figure 1 shows a model of an electromagnetic mill constructed at the Lublin University of Technology and being the subject of this research. According to the current knowledge of the authors, this is the first construction of this type of mill using the stator of an asynchronous motor as inductor. The structure, principle of operation and selected research have been described in literature items [5], [6], [7], [8], [9].

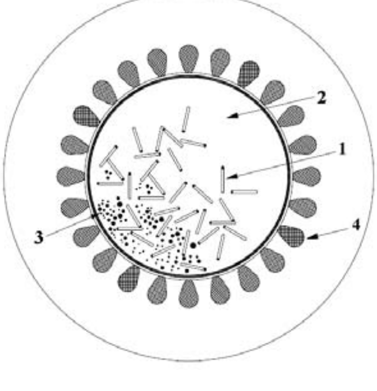

Fig. 1. Electromagnetic mill with latent poles [9]: 1 – grinding media, 2 – working chamber, 3 – material ground, 4 – winding in grooves

The reluctance model of the mill

The development of a comprehensive mathematical model requires a number of simplification assumptions which will be presented when the model is considered.

It has been adopted to describe the mathematical model of the mill in the Cartesian xy system. It follows that the grinding elements are arranged along the electromagnetic field force lines. In practice, the grinding media may be arranged in the z direction (this results from numerous collisions with both the shredded material and other grinding media), but the electromagnetic field of the inductor brings them back to the xy plane.

The considerations started from the simplest case, when there is only one grinding element in the working chamber. The exciter, air gap, working chamber and rotor (grinding element – grinder) are divided into sub-areas perpendicular to the machine axis. It is also assumed that the air areas (outside the air gap) have a reluctance equal to infinity and that the walls of the working chamber have no significant influence on the distribution of electromagnetic field inside the inductor area. Due to the fact that the grinding element moves in the entire diameter of the working chamber and thus in the entire internal diameter of the inductor, the division into sub-areas varies over time, depending on the location of the grinding media. The analysis began with the location of the grinding wheel at the working chamber itself along the force lines of the electromagnetic field (Fig. 2).

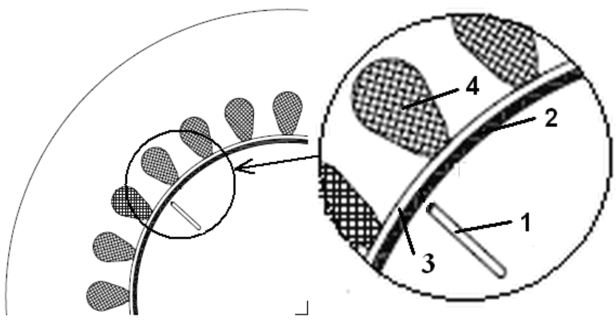

Fig. 2. Fragment of the area analysed: 1 – grinding media (mr – millennium area), 2 – working chamber 1 mm (kr – working chamber area), 3 – air gap 1,5 mm (δr – air gap area), 4 – nursery with windings (rr – inductor area)

The general dependence of the reluctance of magnetic circuit elements depending on geometrical dimensions and magnetic permeability has the following form:

$$R_\mu = \frac{l}{S \cdot \mu} \tag{1}$$

where: R_μ – element reluctance; l – reluctance element length; S – reluctance element cross-sectional area; μ – material magnetic permeability.

In the system analysed the following areas are taken into account: inductor, air gap, working chamber and grinding media in the radial (radial reluctance) and tangential (tangential reluctance) directions reluctance.

Reluctance of inductor teeth in the radial direction:

$$R_{\mu zr} = \frac{l_{zr}}{S_{zsrr} \cdot \mu_{Fezj}} \tag{2}$$

where: l_{zr} – length of the inductor tooth along the radius, S_{zsrr} – mean cross-sectional area of the inductor tooth along the radius, μ_{Fezj} – magnetic permeability of the inductor plates.

Reluctance of the inductor yoke in the tangential direction:

$$R_{\mu j\varphi} = \frac{l_{j\varphi}}{S_{jsr\varphi} \cdot \mu_{Fezj}} \tag{3}$$

where: $l_{j\varphi}$ – length of the inductor yoke along the tangent, $S_{jsr\varphi}$ – mean cross-sectional area of the inductor yoke along the tangent, μ_{Fezj} – magnetic permeability of the inductor plates.

Reluctance of air gap in the radial direction:

$$R_{\mu\delta r} = \frac{l_{\delta r}}{S_{\delta srr} \cdot \mu_\delta} \tag{4}$$

where: $l_{\delta r}$ – length of air gap along the radius, $S_{\delta srr}$ – mean cross-sectional area of air gap along the radius, μ_δ – magnetic permeability of air.

Reluctance of the air gap in the tangential direction:

$$R_{\mu\delta\varphi} = \frac{l_{\delta\varphi}}{S_{\delta sr\varphi} \cdot \mu_\delta} \tag{5}$$

where: $l_{\delta\varphi}$ – air gap length along the tangent, $S_{\delta sr\varphi}$ – mean cross-sectional area of the air gap along the tangent, μ_δ – magnetic permeability of air.

Reluctance of the working chamber in the radial direction:

$$R_{\mu kr} = \frac{l_{kr}}{S_{ksrr} \cdot \mu_k} \tag{6}$$

where: l_{kr} – working chamber length along the radius, S_{ksrr} – average cross-sectional area of the working chamber along the radius, μ_k – magnetic permeability of the working chamber.

Reluctance of the working chamber in the tangential direction:

$$R_{\mu k\varphi} = \frac{l_{k\varphi}}{S_{ksr\varphi} \cdot \mu_k} \tag{7}$$

where: $l_{k\varphi}$ – working chamber length along the tangent, $S_{ksr\varphi}$ – average cross-sectional area of the working chamber along the tangent, μ_k – magnetic permeability of the working chamber.

Reluctance of the grinding media in the radial direction:

$$R_{\mu mr} = \frac{l_{mr}}{S_{msrr} \cdot \mu_{Fer}} \tag{8}$$

where: l_{mr} – length of the grinding media along the radius, S_{msrr} – average cross-sectional area of the grinding media along the radius, μ_{Fer} – magnetic permeability of the grinding media.

Due to the small diameter of the grinding media and the assumption that there is only one grinding element in the system analysed, tangential reluctance of the grinding media does not occur. Due to unpredictable distribution, the crushed material was not taken into account in the considerations.

Figure 3 shows the developed magnetic circuit of the mill with a division into sub-areas developed by the authors. The model was created analogously to the model of a reluctance motor with a rolling rotor described in the literature [10]. It presents a reluctance grid, sample names of selected reluctances and names of grid parameters. Due to the symmetrical character of the device, the separated area occupies a quarter of the whole circuit.

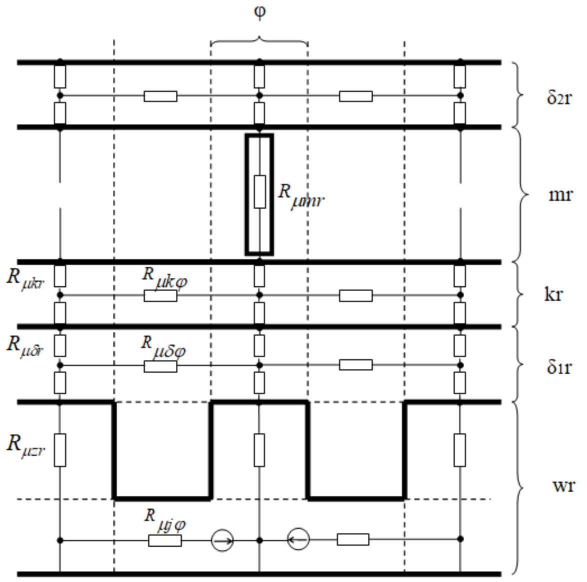

Fig. 3. Developed magnetic circuit of the mill (without proportion): wr – inductor area, δr – air gap area, kr – working chamber area, mr – area of the grinding media, φ –area analysed

The density of sub-areas (of the network) affects the accuracy of calculations. Individual network parameters may have different values. The figure shows that it is possible to link the reluctance value with the size of the network division for:

- radial reluctance of the inductor sub-area:

$$\theta_{wr\varphi r} = \frac{wr}{\varphi}, \tag{9}$$

- radial reluctance of the air gap sub-area:

$$\theta_{\delta r\varphi r} = \frac{\delta r}{\varphi}, \tag{10}$$

- radial reluctance of the sub-area of the working chamber:

$$\theta_{kr\varphi r} = \frac{kr}{\varphi}, \tag{11}$$

- radial reluctance of the grinding sub-area:

(12) $$\theta_{mr\varphi r} = \frac{mr}{\varphi},$$

- reluctance of the tangential sub-area of the inductor:

(13) $$\theta_{wr\varphi\varphi} = \frac{1}{\theta_{wr\varphi r}},$$

- reluctance of the tangential sub-area of the air gap:

(14) $$\theta_{\delta r\varphi\varphi} = \frac{1}{\theta_{\delta r\varphi r}},$$

- reluctance of the tangential sub-area of the working chamber:

(15) $$\theta_{kr\varphi\varphi} = \frac{1}{\theta_{kr\varphi r}},$$

- reluctance of the tangential sub-area of grinding media:

(16) $$\theta_{mr\varphi\varphi} = \frac{1}{\theta_{mr\varphi r}}.$$

The connection was made for the simplest network division θ_{ijk}=1 (for *i,j,k* = 1,2,3...).

By substituting dependencies (9)-(16) under the appropriate reluctance values specified by formulas (2)-(8) and taking into account the geometric dimensions of individual elements, we obtain the final result:

- reluctance of the inductor teeth in the radial direction:

(17) $$R_{\mu zr} = \frac{r_{zw} - r_{ww}}{\mu_{Fezj} \cdot l_b \cdot l_w \cdot \theta_{wr\varphi r}},$$

where: r_{zw} – the external radius of the inductor area in which the magnetic flux flows; r_{ww} – the internal radius of the inductor area in which the magnetic flux flows; l_b – the length of the sheet metal packet; l_w – the width/length of the inductor area in which the magnetic flux flows;

- reluctance of the inductor yoke in the tangential direction:

(18) $$R_{\mu j\varphi} = \frac{l_w}{\mu_{Fezj} \cdot l_b \cdot (r_{zw} - r_{ww}) \cdot \theta_{wr\varphi\varphi}},$$

- reluctance of the air gap in the radial direction:

(19) $$R_{\mu\delta r} = \frac{r_{z\delta} - r_{w\delta}}{\mu_\delta \cdot l_b \cdot l_\delta \cdot \theta_{\delta r\varphi r}},$$

where: $r_{z\delta}$ – the external radius of the air gap area in which the magnetic flux flows; $r_{w\delta}$ – the internal radius of the air gap area in which the magnetic flux flows; l_b – the length of the sheet metal packet; l_δ – the width/length of the air gap area in which the magnetic flux flows;

- reluctance of the air gap in the tangential direction:

(20) $$R_{\mu\delta\varphi} = \frac{l_\delta}{\mu_\delta \cdot l_b \cdot (r_{z\delta} - r_{w\delta}) \cdot \theta_{\delta r\varphi\varphi}},$$

- reluctance of the working chamber in the radial direction:

(21) $$R_{\mu kr} = \frac{r_{zk} - r_{wk}}{\mu_k \cdot l_b \cdot l_k \cdot \theta_{kr\varphi r}},$$

where: r_{zk} – the external radius of the working chamber area in which the magnetic flux flows; r_{wk} – the internal radius of the working chamber area in which the magnetic flux flows, l_b – the length of the sheet metal package; l_k – the width/length of the working chamber area in which the magnetic flux flows;

- reluctance of the working chamber in the tangential direction:

(22) $$R_{\mu k\varphi} = \frac{l_k}{\mu_k \cdot l_b \cdot (r_{zk} - r_{wk}) \cdot \theta_{kr\varphi\varphi}},$$

- reluctance of the grinding media in radial direction:

(23) $$R_{\mu mr} = \frac{r_{zm} - r_{wm}}{\mu_r \cdot \pi \cdot {r_m}^2 \cdot \theta_{mr\varphi r}},$$

where: r_{zm} – the outer radius of the grinding media area in which the magnetic flux flows; r_{wm} – the inner radius of the grinding media area in which the magnetic flux flows; r_m – the grinding medium radius.

In the case where the area contains a larger number of grinding media arranged along the magnetic field force lines, Formula (23) will have the form:

(24) $$R_{\mu mr} = \sum_{m=1}^{n} \frac{r_{zm} - r_{wm}}{\mu_r \cdot \pi \cdot {r_m}^2 \cdot \theta_{mr\varphi r}},$$

where: m, n – number of grinding media.

a)

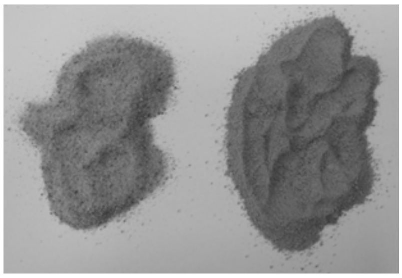

b)

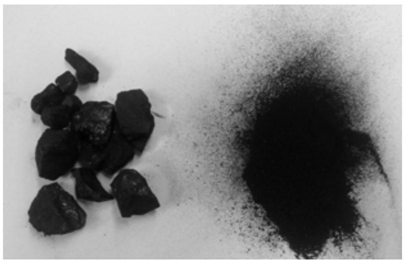

c)

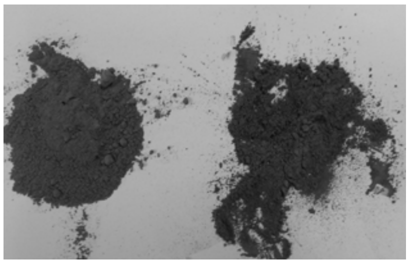

Fig. 4. Raw material before (on the left) and after (on the right) grinding: (a) quartz sand, (b) hard coal, (c) volatile dust

The air gap velocity *δ2r* can be calculated from formulae (19) and (20). If the grinding media are located elsewhere than in the working chamber wall, the size of the air gap above and below the grinding media must be taken into account according to the same formulae.

If multiple pellets are used to calculate the reluctance values of individual elements, the size of the calculation grid should be concentrated and calculations made for each individual pellet. In case of a large number of milling media, their interaction with each other should be taken into account, which demands the calculation of the reluctance of the milling media in the tangential direction.

Efficiency of the mill's operation

There are many meanings behind the concept of an electromagnetic mill's efficiency. The criteria could be the size of the shredded material, short grinding time or low energy consumption. This efficiency depends on many parameters, such as: construction, operation, technology.
Laboratory tests were carried out in order to determine the group of materials (raw materials) that can be crushed. It should be noted that when changing the type of shredded material, it is necessary to select the appropriate size of the grinding media for each type of feed. Examples of grinding effects in an electromagnetic mill are shown in Figure 4.
The granulometric distribution for quartz sand before and after grinding is shown in Figure 5.

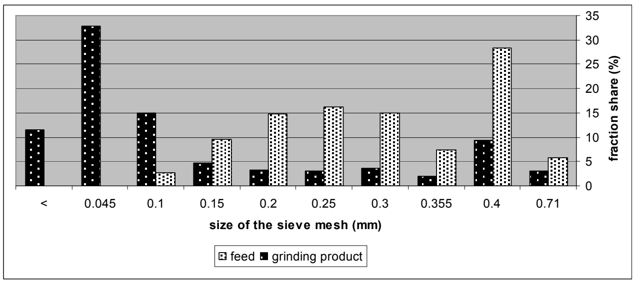

Fig. 5. Grit size distribution before and after grinding in an electromagnetic mill (quartz sand)

Summary

An electromagnetic mill is a device in which the shredded material is exposed to a few force fields. In the working area of this type of devices there is energy in the form of electromagnetic field, which is accompanied by various types of conversion, among others, into kinetic energy, elasticity and heat. Due to the simultaneous influence of electromagnetic and thermal fields, as well as high pressure and friction on the shredded material, it is possible to achieve much better grinding results than using conventional methods. Thanks to these properties, the electromagnetic mill, in addition to grinding various types of materials and raw materials, can be used to mix or grind materials, accelerate certain chemical reactions or activate fly ashes, as well as being employed in mechanical melting processes.

***Authors**: dr inż. Sebastian Styła, Politechnika Lubelska, Instytut Elektrotechniki i Elektrotechnologii, ul. Nadbystrzycka 38A, 20-618 Lublin, E-mail: s.styla@pollub.pl;*
mgr inż. Monika Mańko, Politechnika Lubelska, Instytut Elektrotechniki i Elektrotechnologii, ul. Nadbystrzycka 38A, 20-618 Lublin, E-mail: monika.manko@pollub.edu.pl.

REFERENCES

[1] Binczyk F., Polechoński W., Skrzypek S. J., Piątkowski J., Zastosowanie młyna wysokoenergetycznego do mielenia i mechanicznego stopowania materiałów proszkowych, *Inżynieria Materiałowa*, nr 3-4 (1999), 180-185
[2] Sosiński R., Szczypiorowski A., Szymanek P., Nowak W.: Problematyka zastosowań młyna elektromagnetycznego, XIV Międzynarodowa Konferencja „Popioły z energetyki", Międzyzdroje, 17-19 październik 2007, 95-105
[3] Sławiński, K. Knaś, K. Gandor, M. Balt, B. Nowak, W., Młyn elektromagnetyczny i jego zastosowanie do mielenia i suszenia węgli, *Piece Przemysłowe & Kotły*, t. 1-2 (2014), 21-25
[4] Wołosiewicz-Głąb M., Foszcz D., Gawenda T., Analysis of Possibilities of Obtaining the Fine Particle Size in Mills of Various Designs, *Inżynieria Mineralna*, 17 (2016), no. 1, 223-231
[5] Styła S., Pietrzyk W., Młyn elektromagnetyczny z trójfazowym wzbudnikiem pola wirującego, Patent nr 221027, WUP 2/2016, zgłoszenie patentowe nr. P.395321
[6] Styła S., Examination of an electromagnetic mill structure by means of infrared radiation, *Przegląd Elektrotechniczny*, 90 (2014), no. 3, 179-182
[7] Styła S., Analysis of temperature distribution in electromagnetic mill, *Przegląd Elektrotechniczny*, 92 (2016), no. 3, 103-106
[8] Styła S., A new grinding technology using an electromagnetic mill–testing the efficiency of the process, *ECONTECHMOD: an International Quarterly Journal on Economics of Technology and Modelling Processes*, 6 (2017), no. 1, 81-88
[9] Styła S., Laboratory studies of an electromagnetic mill inductor with a power source, *ECONTECHMOD: an International Quarterly Journal on Economics of Technology and Modelling Processes*, 6 (2017), no. 2, 109-114
[10] Kamiński G., Rogalski A., Model kompleksowy silnika reluktancyjnego przełączalnego z toczącym się wirnikiem, *Prace Naukowe Politechniki Warszawskiej. Elektryka*, z. 116 (2001), 11-47